

Evidence for the exchange effect in the β decay of ^{241}Pu

X. Mougeot,* M.-M. Bé, C. Bisch, and M. Loidl
 CEA, LIST, LNHB, Gif-sur-Yvette, F-91191, France
 (Received 10 July 2012; published 10 October 2012)

The exchange effect has been previously given as a possible explanation for a significant deviation from an allowed shape observed at low energy in the ^{241}Pu β spectrum. Calculations set out here confirm that this atomic effect explains a large part of this deviation. The equations needed to calculate the exchange effect are detailed, as well as the evaluation of the confluent hypergeometric function for complex arguments of large magnitudes. After a review of the possible other effects that could explain the remaining discrepancy at low energy, the screening correction using effective nuclear charges seems to be the best explanation. For radionuclides with high Z , this work has demonstrated the necessity to take into account the spatial variation of the nuclear charge experienced by the ejected electron to accurately correct for the screening effect.

DOI: [10.1103/PhysRevA.86.042506](https://doi.org/10.1103/PhysRevA.86.042506)

PACS number(s): 31.15.-p, 23.40.-s

I. INTRODUCTION

Metallic magnetic calorimetry has been shown to be a powerful experimental technique to study the energy spectra of β particles having a maximum energy of about 1 MeV. Beyond this energy range, the bremsstrahlung effect makes a significant contribution and studies have to be conducted to evaluate the relevance of this technique. The β spectrum of ^{241}Pu was recently measured using a metallic magnetic calorimeter [1]. The source was enclosed in a gold absorber assuring a 4π solid angle and 100% detection efficiency. The energy resolution, 29 eV at 5.9 keV, and the energy threshold, 300 eV, allow one to test the theoretical β spectra calculations with an accuracy never before achieved. The spectrum from [1] has already been compared to classical β calculations [2], and in this framework, a significant deviation of the experimental spectrum below 5 keV could not be explained. The exchange effect has been given as a possible cause, which is explained here in detail.

The radionuclide ^{241}Pu mainly decays by β^- emission to the ground state of ^{241}Am , and the transition probability was evaluated to be $P(\beta^-) = 99.99756(2)\%$, the remaining being α decays [3]. The nature of the transition is first forbidden nonunique, with a maximum available energy of $Q_{\beta^-} = 20.8(2)$ keV. Its half-life $T_{1/2} = 14.33(4)$ yr was evaluated from published measurements which are independent of the β spectrum.

A β spectrum is the product of (i) a weak interaction coupling constant, (ii) a statistical phase space factor which reflects the momentum distribution between the electron and the neutrino, (iii) the so-called Fermi function which corrects for the Coulomb effects, and (iv) a shape factor which contains all the remaining energy dependencies, as leptonic and nuclear matrix elements or atomic effects corrections. A calculation program of the shapes of β spectra was already developed and described elsewhere for allowed and forbidden unique transitions [2]. In this kind of β transition, the energy dependence of the nuclear matrix elements can be factored out. This is not possible for forbidden nonunique transitions,

hence the calculations become more complex. However, first forbidden nonunique transitions which fulfill the assumption $2\xi = \alpha Z/2R \gg E_0$ can be treated as allowed ones [4], with α the fine structure constant, R the radius of the daughter nucleus, Z its nuclear charge, and E_0 the maximum energy of the transition. This approximation, also called the ξ approximation, simply means that the Coulomb energy of the β electron at the nuclear radius must be large compared to the total decay energy. The ^{241}Pu β decay is a case study because of its low maximum energy (20.8 keV) compared to $2\xi \simeq 19.8$ MeV. Therefore, this transition can be calculated as an allowed one.

Atomic effects play an important role in the shape of β spectra, mainly at low energy. Atomic electrons partially screen the nuclear charge seen by the β electron: this is the well-known screening effect. The sudden change of the nuclear charge can induce atomic excitations or internal ionizations, which are respectively called shake-up and shake-off effects and are not expected to have a contribution higher than 0.1%. The exchange effect is also an atomic effect. It arises from the creation of a β electron in a bound orbital of the daughter atom corresponding to one which was occupied in the parent atom. An atomic electron from the bound orbital makes simultaneously a transition to a continuum orbital of the daughter atom. This process cannot be distinguished from the direct decay to a final state containing one continuum electron.

The first study of the exchange effect was only focused on the $1s$ orbital. The conclusion was a destructive interference with the direct process, leading to a lower emission probability at low energy [5]. Twenty years later, a specific study of the exchange effect in the tritium β decay showed an enhancement at low energy, consistent with recent measurements [6]. The theoretical formalism of the exchange effect in the case of the allowed transitions was then extended to higher orbitals, including also the screening effect [7]. It was shown that the exchange effect should systematically enhance the decay probability at low energy.

Qualitative evidence of the exchange effect was first observed by the measurement of the β spectrum of ^{107}Pd with a cryogenic microcalorimeter [8]. A different type of cryogenic detector provided quantitative evidence in the β spectrum of

*xavier.mougeot@cea.fr

^{63}Ni [9], but the contribution of the exchange effect is low above the energy threshold (8 keV). The β decay of ^{63}Ni is well suited for testing the atomic exchange effect because it is an allowed transition, which simplifies the calculations, and because of its low endpoint energy, 66.980 (15) keV [10]. Recently, this spectrum was measured using the same technique as in [1], with an energy threshold of ~ 200 eV [11]. It was shown that the exchange correction factor determined following the formalism from [7] leads to a very good agreement between theory and experiment down to these very low energies.

II. FORMALISM

A. General considerations

The formalism used in this publication is from Harston and Pyper [7]. The exchange effect is expressed as a correction factor which modifies the β spectrum intensity I :

$$\frac{dI}{dE} = \frac{dI^{\text{NE}}}{dE} [1 + \eta_{\text{ex}}^T(E)], \quad (1)$$

where the superscript NE stands for “no exchange,” and $\eta_{\text{ex}}^T(E)$ is the total exchange factor depending on the β electron energy E . The exchange factor must involve the overlap between the electron radial wave functions of the bound and continuum orbitals.

For allowed transitions, only β electrons created into an s bound orbital of the daughter atom take part in η_{ex}^T . Indeed, a β transition is classified by the properties of the initial and final nuclear states: the total angular momentum change ΔJ and the parity change $\Delta\pi$. For an allowed transition, $\Delta J = 0, \pm 1$ and $\Delta\pi = 0$, which means that the electron-neutrino pair does not carry away any orbital angular momentum. Thus, only the ns orbitals are reachable by the β electron.

In the first study of the exchange effect, Bahcall [5] pointed out that in the hydrogenic approximation the probability density of the β electron at the center of the nucleus is

$$|\Psi_{ns}(0)|^2 \propto \pi^{-1} \left(\frac{\alpha Z}{n} \right)^3, \quad (2)$$

with n the principal quantum number and Z the charge of the daughter nucleus. The conclusion was that the largest contribution comes from the $1s$ orbital and the higher orbitals can be ignored. In their extended formalism, Harston and Pyper [7] underlined that the other ns orbitals could have a contribution of the same magnitude at low energy. They also highlighted an inconsistency in the wave functions used in Bahcall’s calculations, giving a destructive interference of the exchange effect with the direct decay. Finally, they predicted an enhancement of about 10% below 5 keV, from $Z = 10$ to $Z = 90$.

B. Expression

The total exchange factor can be written in terms of the subshell contributions η_{ex}^{ns} :

$$\eta_{\text{ex}}^T(E) = \sum_n \eta_{\text{ex}}^{ns}(E) + \sum_{\substack{m,n \\ (m \neq n)}} \mu_m \mu_n, \quad (3)$$

and the exchange factor of the n th subshell is given by

$$\eta_{\text{ex}}^{ns}(E) = f_s (\mu_n^2 - 2\mu_n). \quad (4)$$

The parameters μ_n and f_s are expressed in terms of the bound and continuum electron radial wave functions according to

$$\mu_n = \langle Es' | ns \rangle \frac{g_{n,\kappa}^b(R)}{g_\kappa^c(R)} \quad \text{and} \quad f_s = \frac{g_\kappa^c(R)^2}{g_\kappa^c(R)^2 + f_\kappa^c(R)^2}. \quad (5)$$

All the parameters are explained in the next section.

The second sum in Eq. (3) is not taken into account in [7] because of its expected smallness. Even if this is true over almost the entire energy range of the β spectra, the contribution of this term can be about 1–3% below 1 keV. It was therefore included in the present calculations.

C. Electron radial wave functions

The electron wave function is defined in [12] by its small and large radial components f and g :

$$\Psi_\kappa(\vec{r}) = \begin{pmatrix} g_\kappa(r) \sum_\mu \chi_\kappa^\mu \\ if_\kappa(r) \sum_\mu \chi_{-\kappa}^\mu \end{pmatrix}, \quad (6)$$

where the spin-angular functions χ_κ^μ are expanded into the orthonormal basis of the spherical harmonics $Y_l^{\mu-m}$:

$$\chi_m^\mu = \sum_m C \left(l \frac{1}{2} j; \mu - m, m \right) Y_l^{\mu-m} \chi^m, \quad (7)$$

with the Clebsch-Gordan coefficients C and the two-component spin eigenfunctions χ^m . κ is the eigenvalue of the operator $\hat{K} = \beta(\vec{\sigma} \cdot \vec{L} + 1)$ which appears by applying the theory of angular momentum to an electron in a Coulomb central field: β is the Dirac matrix, $\vec{\sigma}$ designates the Pauli matrices $\sigma_{x,y,z}$ and \vec{L} is the orbital angular momentum operator.

The electron radial wave functions for the bound ($f_{n,\kappa}^b, g_{n,\kappa}^b$) and continuum (f_κ^c, g_κ^c) orbitals are the analytical solutions of the Dirac equation in the hydrogenic approximation given by Rose [12]. With $\kappa = -1$ for s orbitals, the following parameters are defined:

$$\begin{aligned} n' &= n - |\kappa|, & \zeta &= \alpha Z, & \gamma &= \sqrt{\kappa^2 - \zeta^2}, \\ \lambda &= \left[1 + \left(\frac{n' + \gamma}{\zeta} \right)^2 \right]^{-1/2}, \\ W_{n,\kappa} &= \left[1 + \left(\frac{\zeta}{n' + \gamma} \right)^2 \right]^{-1/2}, \\ K &= \frac{(2\lambda r)^{\gamma-1} e^{-\lambda r}}{\Gamma(2\gamma + 1)} \left[\frac{2\lambda^5 \Gamma(2\gamma + n' + 1)}{n'! \zeta (\zeta - \lambda \kappa)} \right]^{1/2}, \\ F_1 &= n'_1 F_1(-n' + 1, 2\gamma + 1, 2\lambda r), \\ F_2 &= (\kappa - \zeta/\lambda)_1 F_1(-n', 2\gamma + 1, 2\lambda r). \end{aligned}$$

The Γ function is the extension of the factorial function to complex numbers. ${}_1F_1$ is the confluent hypergeometric function, whose evaluation is described in Sec. II E. The bound

wave functions are then expressed as

$$f_{n,\kappa}^b = -K\sqrt{1 - W_{n,\kappa}}(F_1 - F_2), \quad (8a)$$

$$g_{n,\kappa}^b = -K\sqrt{1 + W_{n,\kappa}}(F_1 + F_2). \quad (8b)$$

In the same way, the following parameters are defined:

$W = 1 + E/m_e c^2$ the total energy of the electron in rest mass units,

$p = \sqrt{W^2 - 1}$ the corresponding momentum,

$$y = \zeta W/p, Q = \frac{(2pr)^\gamma e^{\pi\gamma/2} |\Gamma(\gamma + iy)|}{2r\sqrt{\pi p} \Gamma(2\gamma + 1)},$$

η is the phase of the wave functions via

$$e^{i\eta} = \left[-\frac{\kappa - iy/W}{\gamma + iy} \right]^{1/2},$$

$$C_1 = e^{-ipr+i\eta} (\gamma + iy)_1 F_1(\gamma + 1 + iy, 2\gamma + 1, 2ipr),$$

$$C_2 = C_1^*.$$

The continuum wave functions are then expressed as

$$f_\kappa^c = iQ\sqrt{W - 1}(C_1 - C_2), \quad (9a)$$

$$g_\kappa^c = Q\sqrt{W + 1}(C_1 + C_2). \quad (9b)$$

The overlap which appears in the left term of Eq. (5) is defined for allowed transitions simply by

$$\langle Es' | ns \rangle = \int_\Omega \Psi_{-1}^{c*}(\vec{r}) \Psi_{-1}^b(\vec{r}) d\Omega. \quad (10)$$

It remains from the spin-angular functions a factor $1/\sqrt{4\pi}$. Thus, integrating over the angular parts and emphasizing the initial and final nuclear charge dependences, one has the explicit form

$$\langle Es' | ns \rangle = \int_{R_{\min}}^{R_{\max}} r^2 [g_{-1}^c(Z_f, r) g_{n,-1}^b(Z_i, r)] dr + \int_{R_{\min}}^{R_{\max}} r^2 [f_{-1}^c(Z_f, r) f_{n,-1}^b(Z_i, r)] dr. \quad (11)$$

D. Effective nuclear charges

When calculating a β spectrum, the screening effect is generally corrected for using a Thomas-Fermi potential which is subtracted from the total energy of the particle [13]. This method creates a nonphysical discontinuity at the minimum energy defined by the potential [2]. This minimum energy is $\lesssim 20$ keV, hence the discontinuity does not generally affect the practical use of the spectrum. Physically the influence of the atomic electrons is expected to be significant when the β wavelength is comparable to the atom size, thus at low energy.

Bahcall [5] and Haxton [6] did not consider the influence of the screening effect in their exchange calculations. Harston and Pyper [7] pointed out that this approximation was not valid for many-electron atoms since the screening distorts the β wave functions and can contribute significantly to the overlap involved. Instead of a Thomas-Fermi potential, they preferred to use effective nuclear charges, also best suited for bound wave functions. Obviously, this does not concern wave functions evaluated at the nuclear radius, for which the full nuclear charge has to be used.

TABLE I. Calculated effective nuclear charges compared to those in [7] for the $^{106}\text{Ru} \rightarrow ^{106}\text{Rh}$ β decay. Δ is the difference.

No.	Z_i ([7])	Z_i	Δ (%)	Z_f ([7])	Z_f	Δ (%)
1	43.322	43.3226	0.001	44.320	44.3210	0.002
2	39.841	39.8412	0.0005	40.819	40.8188	0.0005
3	32.765	32.7656	0.002	33.727	33.7229	0.012
4	22.841	22.7408	0.44	23.866	23.5974	1.1
5	9.5087 ^a	9.67195	1.7	10.620 ^a	9.88093	7.5

^aValues extrapolated from the lower orbitals.

The effective nuclear charge Z_{eff} is equal to the number of protons Z in the nucleus decreased by the electron density integral in a sphere of radius r :

$$Z_{\text{eff}}(r) = Z - 4\pi \times 2 \sum_{nlm} \int_0^r |\Psi_{nlm}(r')|^2 r'^2 dr'. \quad (12)$$

It is difficult to account for the spatial dependency in a simple model. Using the hydrogenic approximation framework, Harston and Pyper calculated effective nuclear charges for each atomic orbital from the mean radius of the orbital. In the nonrelativistic case, the relation is well known:

$$\langle r \rangle = \frac{3n^2}{2Z_{\text{eff}}} - \frac{l(l+1)}{2Z_{\text{eff}}}. \quad (13)$$

As only s orbitals have to be considered, $l = 0$. For medium and large Z , a relativistic relation is needed [14]:

$$\langle r \rangle = \frac{(n' + \gamma)(3N^2 - \kappa^2) - \kappa N}{2NZ_{\text{eff}}}, \quad (14)$$

with $N = \sqrt{(n' + \gamma)^2 + \zeta^2}$.

According to Eq. (13) or (14), Harston and Pyper calculated the mean radii in the Hartree-Fock or the Dirac-Fock approximation using the GRASP code [15]. Atomic data tables including mean radii were preferred in this study. Within the Hartree-Fock approximation, values are available up to $Z = 86$ in [16], and up to $Z = 102$ in [17]. They are available up to $Z = 120$ in [18] within the Dirac-Fock approximation. From these tabulated values, the effective nuclear charges were determined for the ^{106}Ru decay (Table I) and for the ^{241}Pu decay (Table II). These compare well with the ones calculated by Harston and Pyper [7] for the first orbitals. The discrepancies for the higher orbitals come from the fact that neutral atoms were assumed in the atomic data tables used

TABLE II. Calculated effective nuclear charges compared to those in [7] for the $^{241}\text{Pu} \rightarrow ^{241}\text{Am}$ β decay. Δ is the difference.

No.	Z_i ([7])	Z_i	Δ (%)	Z_f ([7])	Z_f	Δ (%)
1	93.222	93.2188	0.003	94.213	94.2188	0.006
2	90.485	90.4844	0.0007	91.505	91.5039	0.001
3	84.050	84.0488	0.001	85.108	85.1074	0.0007
4	72.601	72.5986	0.003	73.695	73.6914	0.005
5	56.388	56.3633	0.044	57.527	57.4670	0.11
6	37.452	36.9865	1.3	38.860	37.7924	2.8
7	13.0883 ^a	16.4458	20.4	14.6624 ^a	16.6616	12

^aValues extrapolated from the lower orbitals.

here, whereas Harston and Pyper assumed ions Ru^{1+} , Rh^{2+} , Pu^{3+} , and Am^{4+} .

E. Calculation of the confluent hypergeometric function

The evaluation of the confluent hypergeometric function is the main technical difficulty in the calculation of the exchange effect. The evaluation of ${}_1F_1(a, b, z)$ is required for both cases of bound and continuum wave functions. The parameters required for the calculation of the bound wave functions are $a = -n' + 1$ or $a = -n'$, with $a \in \mathbb{N}$; $b = 2\gamma + 1$, with $b \in \mathbb{R}$; and $z = 2\lambda r$, with $z \in \mathbb{R}$. Those required for the continuum wave functions are $a = \gamma + 1 + iy$; $b = 2\gamma + 1$ (as above); and $z = 2ipr$. Since only s waves contribute to the exchange effect for the allowed transitions, then $\gamma \in]0, 1[$, $b \in]1, 3[$, $\text{Re}(a) \in]1, 2[$. $\text{Im}(a)$ has an energy dependence, e.g., for $Z = 100$, $\text{Im}(a) \simeq 36.9$ at 100 eV and tends to the fine structure constant at high energy. The parameter z is in an open interval. If the endpoint energy of a β spectrum is less than 10 MeV, r might need to be as high as 10^4 (in atomic units) in order to achieve a good accuracy on the overlap calculation. Many methods were tested for the evaluation, the most precise of which were retained and are presented below.

1. Definition

The confluent hypergeometric function is a solution of the Kummer's differential equation

$$z \frac{d^2 u(z)}{dz^2} + (b - z) \frac{du(z)}{dz} - au(z) = 0, \quad (15a)$$

and is defined by the following series:

$${}_1F_1(a, b, z) = \sum_{n=0}^{\infty} \frac{(a)_n z^n}{(b)_n n!}, \quad (15b)$$

where a , b , and z are complex numbers, and $(a)_n$ is the Pochhammer factorial

$$(a)_n = a(a+1)(a+2) \cdots (a+n-1) = \frac{\Gamma(a+n)}{\Gamma(a)}. \quad (15c)$$

The numerical calculation of ${}_1F_1$, especially for complex arguments of large magnitudes, is poorly documented. There is no efficient calculational method available for all possible values of the parameters. A direct calculation is not possible because very large numbers are needed, whose products and ratios give a small quantity. The precision limit of the calculations is quickly achieved, even in double precision.

2. Generalized Laguerre polynomials

For the bound wave functions, an exact solution exists in terms of generalized Laguerre polynomials:

$$L_n^\alpha(x) = \frac{(\alpha+1)_n}{n!} {}_1F_1(-n, \alpha+1, x), \quad (16a)$$

satisfying the recurrence relation

$$L_n^\alpha(x) = \left(2 + \frac{\alpha-1-x}{n}\right) L_{n-1}^\alpha(x) - \left(1 + \frac{\alpha-1}{n}\right) L_{n-2}^\alpha(x), \quad (16b)$$

with the first two polynomials

$$L_0^\alpha(x) = 1, \quad L_1^\alpha(x) = -x + \alpha + 1. \quad (16c)$$

This method allows an exact and quick calculation. Even for $Z = 120$, no orbital beyond $8s$ needs to be considered.

3. Taylor and asymptotic series

The Taylor series method, based on Eq. (15b), defines $A_j = \frac{(a)_j}{(b)_j j!}$ and S_j as the sum of the first j terms of the series, which leads to the following recurrence relations:

$$A_{j+1} = A_j \frac{a+j}{b+j} \frac{z}{j+1}, \quad S_{j+1} = S_j + A_{j+1}, \quad (17)$$

with $S_0 = A_0 = 1$. This method is convenient for complex arguments with small magnitudes, but it quickly diverges.

For larger magnitudes, the asymptotic series method is more appropriate and is defined by

$${}_1F_1(a, b, z) \sim \frac{\Gamma(b)}{\Gamma(a)} e^z z^{a-b} \sum_{j=0}^{\infty} (b-a)_j (1-a)_j \frac{z^{-j}}{j!} + \frac{e^{i\pi a} z^{-a}}{\Gamma(b-a)} \sum_{j=0}^{\infty} (a)_j (1+a-b)_j \frac{(-z)^{-j}}{j!}. \quad (18)$$

Each of the two series in the right term of Eq. (18) is calculated using the Taylor series method described above.

Once again the use of double precision is not sufficient because sometimes, and especially for the higher orbitals, the Taylor series diverges before the asymptotic series converges.

4. CONHYP and iRRAM: Beyond double precision

CONHYP is a FORTRAN numerical evaluator of ${}_1F_1$ for complex arguments of large magnitudes [19]. Extended precision subroutines using large arrays allow calculations with a high accuracy. CONHYP was successfully tested up to magnitudes of about 1000, but the calculation of the exchange effect often needs larger values, for which some limitations are binding. For a better compatibility with our code, it was translated into C++ and the limitations for small and large numbers ($10^{\pm 75}$) and maximal length of arrays (777) were removed. Unfortunately, this program cannot return any value for very large magnitudes, e.g., for the calculation of η_{ex}^{6s} in ^{241}Pu .

iRRAM is a C++ package for error-free real arithmetic [20]. The accuracy of the calculations is only limited by the size of computer memory. Common mathematical functions are defined for three specific data types (INTEGER, REAL, COMPLEX), which allow the package to be easily used. The accuracy of the calculation is controlled by redefining the standard outputs. The main drawback is the necessity to deal with memory instabilities.

The quick divergence of the generalized Laguerre polynomials leads us to calculate them exactly using the iRRAM package. In other cases, the following strategy was adopted for the evaluation of ${}_1F_1$: with iRRAM, use of (i) the Taylor series method for $|z| < 100$ and (ii) the asymptotic series method for $|z| > 100$; (iii) use of CONHYP if no value is returned due to a memory problem.

5. A faster, simpler but less accurate method

Another method should be mentioned, which uses directly the asymptotic solutions of the electron wave functions given in [12]:

$$f = -\left(\frac{W-1}{\pi p}\right)^{1/2} \frac{\sin(pr+\delta)}{r}, \quad (19a)$$

$$g = \left(\frac{W+1}{\pi p}\right)^{1/2} \frac{\cos(pr+\delta)}{r}. \quad (19b)$$

The phase δ is defined by

$$\delta = y \log 2pr - \arg \Gamma(\gamma + iy) + \eta - \pi\gamma/2. \quad (19c)$$

Thus, the evaluation of the confluent hypergeometric function is avoided for large pr values. For small pr values, ${}_1F_1$ was calculated using the Taylor series method in double precision. It turned out that a criterion to switch from the latter method to the former is very difficult to set, since it may be correct for certain orbitals and certain radionuclides, but not consistently. Moreover, one has to check with a more exact calculation, which makes this method inappropriate.

III. RESULTS

Calculations were made initially for the two β decays described in detail by Harston and Pyper: ^{106}Ru and ^{241}Pu . If the same orbitals and the same effective nuclear charges are used, the results from [7] are well reproduced. Figure 1 shows the total exchange factor for the ^{241}Pu decay, with the contribution of each orbital. The $7s$ orbital was included, as described later. The second term in Eq. (3) is also included in our calculation. Its contribution is $\sim 1.2\%$ at 100 eV and decreases quickly with increasing energy.

Theoretical allowed β spectra, calculated with and without exchange effect, were compared to the measured spectrum

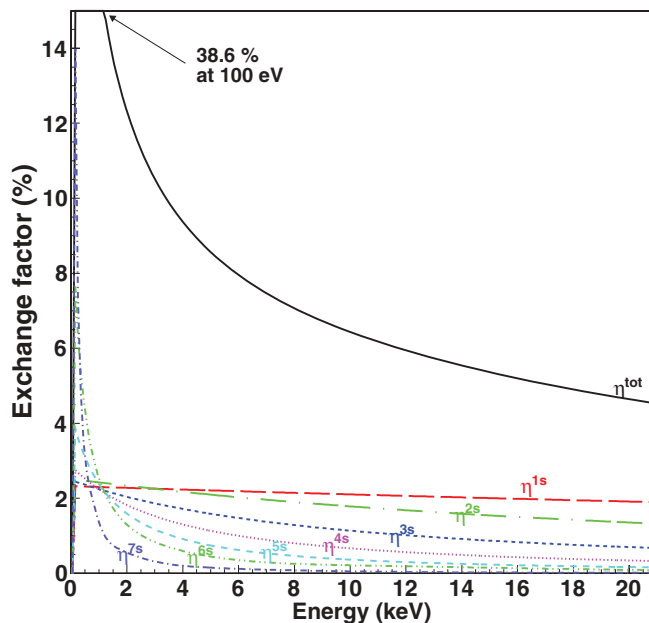


FIG. 1. (Color online) Total exchange factor for the ^{241}Pu β decay and contributions of each orbital. The effective nuclear charges used are the relativistic ones from Harston and Pyper [7] (see Table II).

TABLE III. Integration limits and steps for the radial part used in the calculation of the total exchange factor of the ^{241}Pu β decay.

No.	1	2	3	4	5	6	7
R_{\max}	45	90	150	250	500	900	2700
r step	0.05	0.05	0.1	0.1	0.2	0.2	1

of ^{241}Pu from [1]. The theoretical spectra were normalized to the data in the energy range 7–18 keV. The calculation of the total exchange factor was carried out using the effective nuclear charges given in Table II. Our hypothesis of a neutral atom led us to consider the $7s$ orbital, which has a significant contribution below 1 keV. The integration limits and steps used for the radial part in the calculation of the overlap (11) are given in Table III. The main contribution to the overlap comes from the product of the large radial components of the wave functions. Thus, R_{\max} was chosen such that the amplitude of this product was $\lesssim 10^{-12}$ to ensure an overlap precision of $\sim 10^{-4}$ with $r \sim 10^4$, and the r step was maximized such that a lower step yields an overlap change $\lesssim 10^{-4}$. Figure 2 shows the effect of the complete calculation.

Figure 3 presents the residuals relative to the allowed spectrum without exchange effect for the measured spectrum from [1]. Our calculation—neutral Pu atom with seven orbitals (red solid line)—and the one from [7]—Pu $^{3+}$ ion with six orbitals (green long-dashed line)—are included and give very similar results. We have obtained a better agreement with the experimental spectrum adding the $7s$ orbital to Harston and Pyper's calculation. The result of this calculation is also included in Fig. 3 (blue dot-dashed line). The effective nuclear charge of

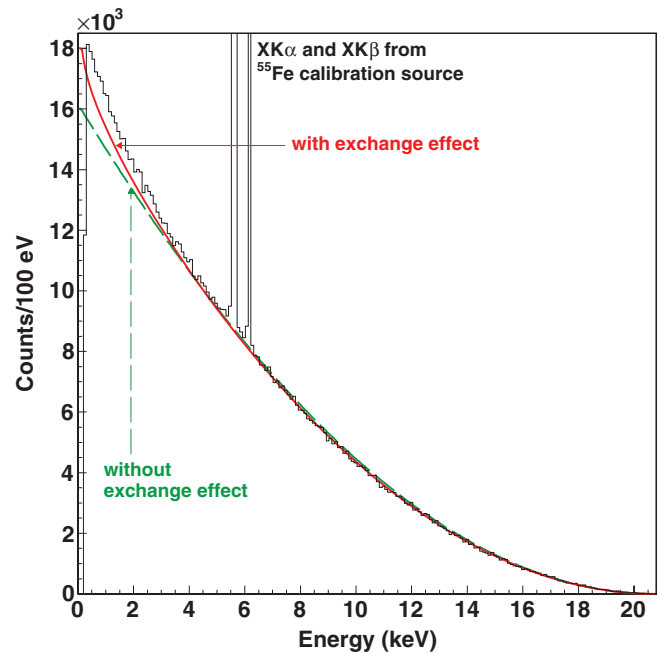


FIG. 2. (Color online) Comparison between the measured β spectrum of ^{241}Pu from Loidl *et al.* [1] and an allowed spectrum calculated with and without exchange effect. The effective nuclear charges used are the relativistic ones calculated for a neutral Pu atom (see Table II).

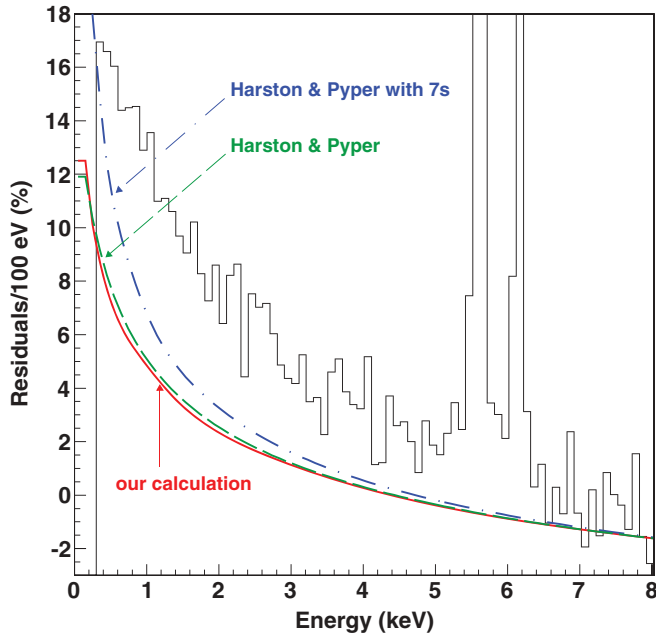


FIG. 3. (Color online) Residuals relative to the allowed spectrum for the measured spectrum of ^{241}Pu from Loidl *et al.* [1], for our calculation including the exchange effect (red solid line), for the one from Harston and Pyper [7] (green long-dashed line), and for the latter one including the $7s$ orbital (blue dot-dashed line). The details of the calculations are explain in the text.

the $7s$ orbital was determined with a second-order polynomial fit from the lower orbitals, and is given in Table II. Obviously, the $7s$ orbital is not filled in the case of a Pu^{3+} ion and should not have to be taken into account. It is just a way of simulating another effect, which is discussed in the next section.

IV. DISCUSSION

The significant deviation from an allowed shape observed at low energy in the ^{241}Pu β spectrum is reproduced in large part by taking into account the exchange effect. But many effects, as described below, are not taken into account in the calculation, which could explain the remaining discrepancy.

(a) *Quality of the measurement.* Commonly used in ionizing radiation metrology for activity measurements, the liquid scintillation counting (LSC) technique requires the knowledge of the spectrum shape in the case of β emitters [21]. The influence of this shape was studied in detail in the case of ^{241}Pu decay [22]. The authors demonstrated that when the shape measured in [1] is used, LSC activity results are in better agreement with results obtained by techniques which are independent of the spectrum shape. The study underlines the quality of the ^{241}Pu β spectrum from [1]. However, the remaining discrepancy at low energy could be due to the measurement itself. For example, the influence of the quality of the source was not yet studied in [1] and could yield distortion effects. This point must be clarified.

(b) *Contribution from the ^{241}Am decay.* One might think the conversion and Auger electrons from the ^{241}Am α decay could have a great influence at low energy, because of their high emission probabilities [23]. However, these electrons are

emitted immediately after the α decay, and the α particle deposits so much energy that the detection system becomes saturated. Thus, this kind of event was easily rejected during the data analysis and the corresponding secondary electrons were not seen. Additionally, the ^{241}Pu source was purified during the preparation and the activity was about 8 Bq for a total acquisition time of 61 h, and as the $T_{1/2}(^{241}\text{Am}) = 432.6(6)$ yr, the ^{241}Am decays were extremely rare.

(c) *Compton background.* Another influence at low energy could be the Compton background from the $K\alpha$ and $K\beta$ X rays of the ^{55}Fe calibration source. The total count in the two peaks is $N(K\alpha + K\beta) \simeq 143\,500$. For gold, the ratio of the photoelectric cross section to the Compton cross section at 5 keV is $\sim 10^6$. Thus, the Compton effect contributes no more than 0.002% which is completely insufficient to explain the remaining discrepancy.

(d) *Theoretical shape factor.* The ^{241}Pu decay is considered as an allowed transition, whereas it is a first forbidden nonunique transition. The accuracy of the ξ approximation is $\sim 1/\xi$, better than 1% in the present case. Moreover, the theoretical shape factor of this transition was already studied through complete calculation of the nuclear matrix elements [24]. Its influence increases linearly with the energy, not higher than 0.3% at the endpoint and 0.1% below 8 keV. Thus, the remaining discrepancy cannot be explained by the allowed transition hypothesis.

(e) *Chemical environment.* The decaying atom is embedded in a chemical environment and the other atoms have an influence on the most external orbitals. A recent measurement of the ^{63}Ni allowed β decay with a metallic magnetic calorimeter can be mentioned as an example [11]. This radionuclide was electroplated on a gold absorber, ensuring a metallic form. Thus, it can be considered as a neutral atom. The spectrum calculation including the exchange effect exhibits an excellent agreement.

In the present case, the β spectrum from [1] might be sensitive to chemical effects due to the accuracy of the measurement and the low energy threshold. However, the chemical composition of the ^{241}Pu source was not clear, being probably a mixture of PuO_2 with a small quantity of $\text{Pu}(\text{NO}_3)_4$. Harston and Pyper estimated that chemical effects cannot be higher than 0.3% by studying different ionic charges [25]. Indeed, Pu has the same oxidation number in PuO_2 as in Pu^{4+} .

As it has been shown in the previous section with the analysis of Fig. 3, the calculated total exchange factor is very similar whether a neutral atom (red solid line) or an ion (green long-dashed line) is considered. Thus, ionic charges might not be the correct approach to simulating chemical effects, because the neutral atom hypothesis yields the same result. A more comprehensive study should consider molecular orbitals, following, for example, the formalism developed in [26].

(f) *Screening.* High- Z nuclides, such as ^{241}Pu , require complete calculation of the effective nuclear charges, taking into account their spatial variations. This was already done for some nuclides 15 yr ago using the Dirac-Fock formalism [27]. The authors calculated the mean energy in the β decay with and without an exchange effect. Among the studied nuclides, they gave results for ^{63}Ni and ^{241}Pu decays.

For ^{63}Ni , we compare our theoretical calculations with the experimental spectrum measured in [11]. Taking the exchange

effect into account led to a mean energy lower by 2.3% than the one without exchange effect. This is in good agreement with the measured result and also with the calculations carried out in [27]. Indeed, the screening correction is weak for such a low- Z nuclide.

For ^{241}Pu , we calculate a mean energy lower by 2.5% taking the exchange effect into account, significantly different from the 4.6% obtained in [27]. The mean energy of the β spectrum from [1] is lower by 3.9% than the calculated one without exchange effect. This fact demonstrates our underestimation of the screening effect for high Z .

Assuming the measured ^{241}Pu spectrum from [1] as definitive, the remaining discrepancy at low energy seems to come from the screening correction more than any other effect. Then, the influence of the screening on the exchange effect must be studied, preferably using the Dirac-Fock formalism, which is beyond the scope of this study.

V. CONCLUSION

All the equations that are necessary to calculate the total exchange factor for allowed β transitions have been presented. The technical difficulty of the evaluation of the confluent hypergeometric function has been set out in detail. From the results shown above, the influence of the exchange effect on

the spectrum shape is demonstrated in the case of low-energy β transitions, especially for ^{241}Pu decay.

However, the exchange effect does not seem sufficient to reproduce well the β spectrum from [1] at low energy. The influence of possible other effects has been reviewed. The evaluation of the chemical effects by Harston and Pyper [25] has been shown to be questionable, but these are not expected to be sufficient enough even considering molecular orbitals. Furthermore, this work has demonstrated that the exchange correction is very sensitive to the screening, which seems to be underestimated by our use of effective nuclear charges. For radionuclides with high Z , it will be necessary to take into account the spatial variation of the nuclear charge experienced by the ejected electron, using electron radial wave functions generated in the Dirac-Fock formalism.

This study also highlights the necessity of a new measurement of the ^{241}Pu β spectrum. As mentioned in [1], an implantation of ^{241}Pu ions directly into the detector absorber is planned in order to limit the influence of the quality of the source.

ACKNOWLEDGMENTS

We warmly thank Robert Vatin and Mark A. Kellett for fruitful discussions.

-
- [1] M. Loidl, M. Rodrigues, B. Censier, S. Kowalski, X. Mougeot, P. Cassette, T. Branger, and D. Lacour, *Appl. Radiat. Isot.* **68**, 1460 (2010).
- [2] X. Mougeot, M.-M. Bé, V. Chisté, C. Dulieu, V. Gorozhankin, and M. Loidl, in *LSC2010, International Conference on Advances in Liquid Scintillation Spectrometry*, edited by P. Cassette (University of Arizona, Tucson, 2010), p. 249.
- [3] M.-M. Bé, V. Chisté, C. Dulieu, E. Browne, V. Chechev, N. Kuzmenko, F. Kondev, A. Luca, M. Galán, A. Pearce, and X. Huang, in *Table of Radionuclides, Monographie BIPM-5*, Vol. 4, edited by CEA/LIST-LNHB (BIPM, Sevres, France, 2008), p. 259.
- [4] H. F. Schopper, *Weak Interactions and Nuclear β Decay* (North-Holland, Amsterdam, 1966).
- [5] J. N. Bahcall, *Phys. Rev.* **129**, 2683 (1963).
- [6] W. C. Haxton, *Phys. Rev. Lett.* **55**, 807 (1985).
- [7] M. R. Harston and N. C. Pyper, *Phys. Rev. A* **45**, 6282 (1992).
- [8] M. M. Lowry, D. Deptuck, and I. C. Girit, *J. Low Temp. Phys.* **93**, 239 (1993).
- [9] L. C. Angrave, N. E. Booth, R. J. Gaitskell, G. L. Salmon, and M. R. Harston, *Phys. Rev. Lett.* **80**, 1610 (1998).
- [10] M.-M. Bé, V. Chisté, C. Dulieu, E. Browne, C. Baglin, V. Chechev, N. Kuzmenko, R. Helmer, F. Kondev, D. MacMahon, and K. B. Lee, in *Table of Radionuclides, Monographie BIPM-5*, Vol. 3, edited by CEA/LIST-LNHB (BIPM, Sevres, France, 2006), p. 29.
- [11] C. Le-Bret, P. Cassette, M. Loidl, X. Mougeot, and M. Rodrigues (unpublished).
- [12] M. E. Rose, *Relativistic Electron Theory* (Wiley, New York, 1961).
- [13] R. H. Good, *Phys. Rev.* **94**, 931 (1954).
- [14] R. H. Garstang and D. F. Mayers, *Proc. Cambridge Philos. Soc.* **62**, 777 (1966).
- [15] K. G. Dyall, I. P. Grant, C. T. Johnson, F. A. Parpia, and E. P. Plummer, *Comput. Phys. Commun.* **55**, 425 (1989).
- [16] C. F. Fischer, *The Hartree-Fock Method for Atoms* (Wiley, New York, 1977).
- [17] J. B. Mann, *At. Data Nucl. Data Tables* **12**, 1 (1973).
- [18] J. P. Desclaux, *At. Data Nucl. Data Tables* **12**, 311 (1973).
- [19] M. Nardin, W. F. Perger, and A. Bhalla, *Trans. Math. Software* **18**, 345 (1992).
- [20] N. T. Müller, in RNC3: Third Conference on Real Numbers and Computers, 1998, p. 13 (unpublished).
- [21] R. Broda, P. Cassette, and K. Kossert, *Metrologia* **44**, S36 (2007).
- [22] W. M. van Wyngaardt, B. R. S. Simpson, M. J. van Staden, and J. Lubbe, *Appl. Radiat. Isot.* **70**, 2188 (2012).
- [23] M.-M. Bé, V. Chisté, C. Dulieu, X. Mougeot, E. Browne, V. Chechev, N. Kuzmenko, F. Kondev, A. Luca, M. Galán, A. L. Nichols, A. Arinc, and X. Huang, in *Table of Radionuclides, Monographie BIPM-5*, Vol. 5, edited by CEA/LIST-LNHB (BIPM, Sevres, France, 2010), p. 175.
- [24] J. Rizek, M. Rysavy, and V. Brabec, *Czech. J. Phys.* **45**, 477 (1995).
- [25] M. R. Harston and N. C. Pyper, *Phys. Rev. Lett.* **56**, 1790 (1986).
- [26] A. Saenz and P. Froelich, *Phys. Rev. C* **56**, 2132 (1997).
- [27] I. M. Band, M. A. Listengarten, and M. B. Trzhaskovskaya, *Bull. Acad. Sci. USSR, Phys. Ser.* **51**, No. 11, 112 (1987).